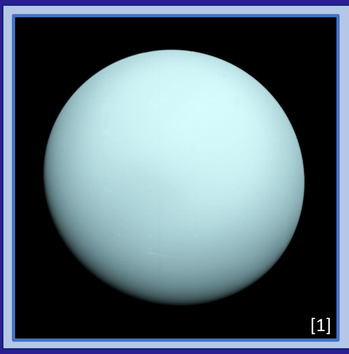
[1]

The unusual radiation belts of the ice giant planets: Getting ready for a future mission

By Charalambos Ioannou and Nick Rayns Supervisor: Dr Adam Masters Research group: Space and Atmospheric Physics

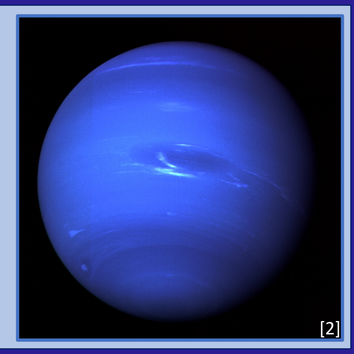
[2]

1 Abstract

- Voyager 2 found a proton intensity in the radiation belts of Uranus and Neptune below the expected level.
- Hypothesis: The large quadrupole moments in the magnetic fields of Uranus and Neptune cause the unusual behaviour.
- We created a test particle simulation to investigate.
- Results indicate that protons experience larger radial drift than electrons in a field with a large quadrupole moment, providing a possible explanation for the proton distribution at the ice giants.

2 Background and Motivation

- In 1986 and 1989, Voyager 2 performed flybys of Uranus and Neptune respectively, and particle intensity was measured.
- Particle spectral intensities in radiation belts are expected to reach the Kennel-Petschek (KP) limit; a limit on maximum particle intensity [3]. At this limit, $\frac{C_m}{C_K} = 1$ (see figure 2).
- Electron intensities reach the limit at Uranus and partly reach it at Neptune [4].
- Proton intensities lie well below the limit at both Uranus and Neptune [5].
- Both Uranus and Neptune have large quadrupole moments in their magnetic fields, and by modelling this field and injecting particles, we hope to find differing behaviour in the electrons and protons to explain this unusual deficit.

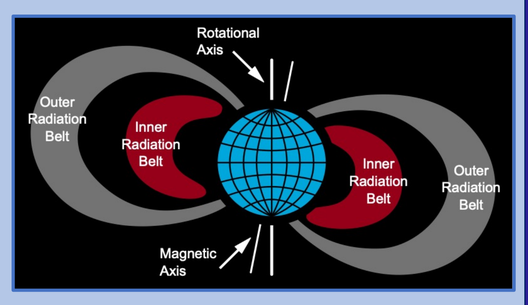

Figure 1: A diagram of the radiation belts of Earth. These are regions where charged particles trapped by the planetary magnetic field accumulate. Image sourced from [6].

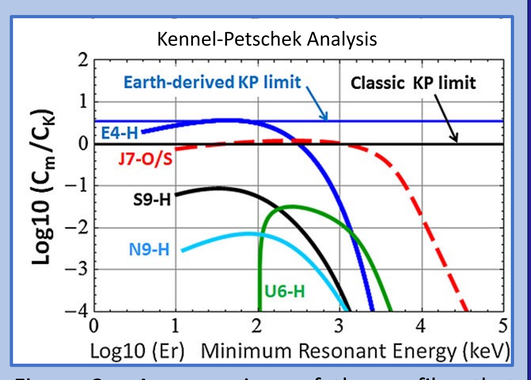

Figure 2: A comparison of the profiles that result from a KP analysis of ion spectra at Earth (E), Jupiter (J), Saturn (S), Uranus (U) and Neptune (N). The number following the planet letter gives the approximate L-shell where the results were recorded. Both the Uranus and Neptune spectra reside below the KP limit. Image adapted from [5].

3 Quadrupole VS Dipole Fields

- In the absence of local currents ($\nabla \times \boldsymbol{B} = 0$), the magnetic field can be expressed as the gradient of a scalar potential, V ($\boldsymbol{B} = -\nabla V$). V can be expanded in a series of functions known as the spherical harmonics, such that

$$V = a \sum_{n=1}^{\infty} \left\{ \left(\frac{r}{a}\right)^n T_n^e + \left(\frac{a}{r}\right)^{n+1} T_n^i \right\}$$

where a is the equatorial radius of the planet and T_n^e and T_n^i are series representing the contributions due to external and internal sources, respectively. The external contributions are truncated to $N = 1$, corresponding to a uniform field. From this expression the components of the magnetic field can be determined. The $n = 1$ and $n = 2$ terms are associated with the dipole and quadrupole components of the magnetic field, respectively. [7]

- Using the data from Voyager 2, the dipole and quadrupole components of the ice giants' magnetic fields were calculated by F. Herbert [8], based on the spherical harmonic model.
- The ratio between the quadrupole and dipole moments was calculated, and characteristic locations where the magnetic field deviated from that of a dipole were determined.
- The direction of the curvature drift experienced by a particle along an L shell was determined to observe if the particles would drift radially across L shells.

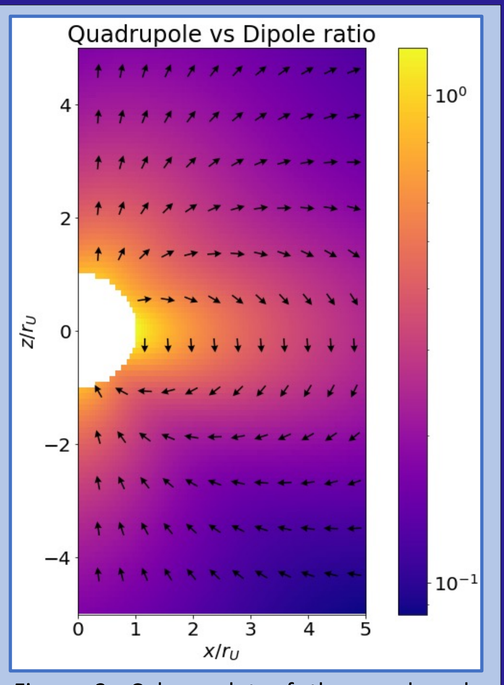

Figure 3. Colour plot of the quadrupole against dipole ratio of the magnetic field of Uranus. A high value indicates a strong quadrupole component. The arrows indicate the combined dipole and quadrupole magnetic field of the planet.

The **L shell** value describes the magnetic field lines that cross the planet's magnetic equator at L planetary radii away from its centre.

Total Drift Velocity

$$\boldsymbol{v}_C = \frac{m}{2qB}\left(v_\perp^2 + 2v_\parallel^2\right)\frac{\boldsymbol{B}\times\nabla B}{B^2}$$

Internal Sources Contribution

$$T_n^i = \sum_{m=0}^{n} \{P_n^m(\cos\theta) [g_n^m \cos m\varphi + h_n^m \sin m\varphi]\}$$

Where $P_n^m(\cos\theta)$ are the Legendre functions

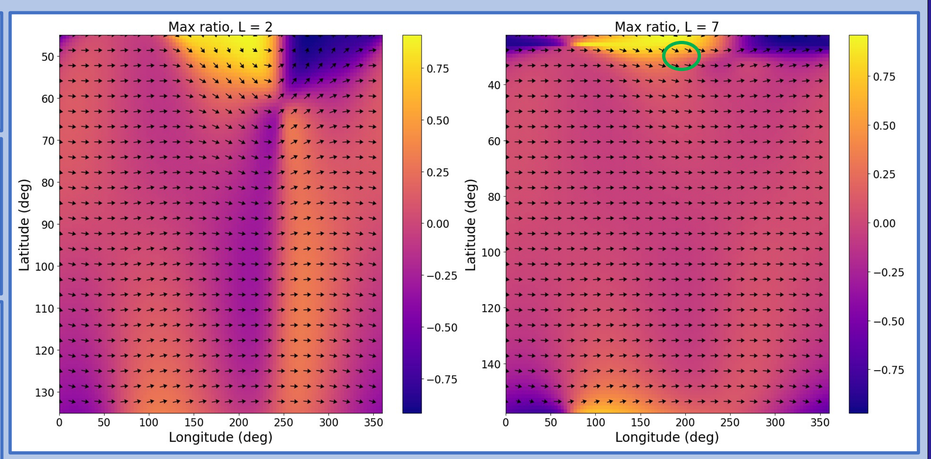

Figure 4. Normalised total drift velocity direction for L shells 2 and 7 of Uranus. The colour plot indicates the radial drift experienced by the particle. Positive values are directed towards the planet for a particle with positive charge. In contrast to the dipole field case, particles experience significant radial drift, especially at latitudes close to the poles. Particles in our simulation were made to reflect at the region marked by the green circle, with coordinates $L = 7$, $\theta = 30°$ and $\varphi = 200°$.

4 Simulations

- To test our hypothesis we developed a test particle numerical scheme based on a paper by Soni *et al* [9].
- The scheme follows a sixth order Runge-Kutta algorithm solving the relativistic equation of motion of a charged particle:

$$\gamma m_0 \frac{\mathrm{d}\boldsymbol{v}}{\mathrm{d}t} = q\boldsymbol{v}\times\boldsymbol{B}$$

$$\boldsymbol{v} = \frac{\mathrm{d}\boldsymbol{r}}{\mathrm{d}t}$$

- To validate our numerical scheme, we ran simulations of a proton's trajectory in a uniform and dipole field, making sure that the energy and adiabatic invariant remained constant.

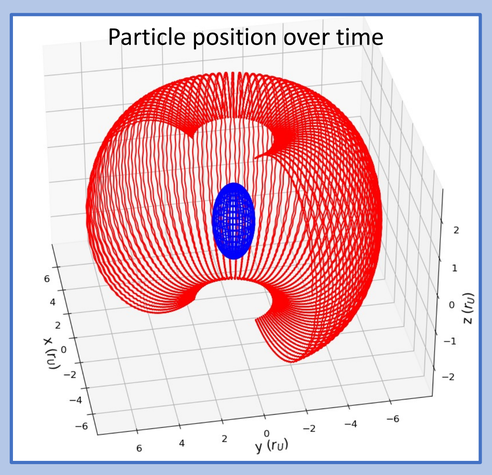

Figure 5. Simulation of a 1MeV proton in the dipole only field of Uranus.

- A long-duration run was performed using the complete field of Uranus and the dipole-only component as a control.
- Multiple short tests were also performed focussing on launching particles into regions of large radial drift. Change in equatorial radial position after one bounce was recorded. For a dipole field, no change would be expected.
- Tests for both electrons and protons with energies between 1keV – 10MeV were performed in order to test our hypothesis.

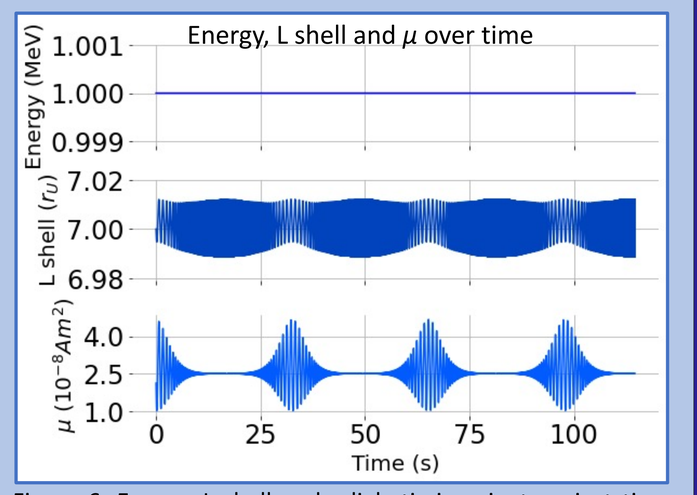

Figure 6. Energy, L shell and adiabatic invariant against time for a 1 MeV proton in a dipole field. The variation in μ and L are due to the gyromotion of the proton.

5 Results

Initial Long Run

- Large deviations in particle L-shell were found in the case of the complete field, but not in the dipole case (see figure 7), indicating the quadrupole component is causing drift between L-shells.
- To break this down further, we consider single reflections at the pole.

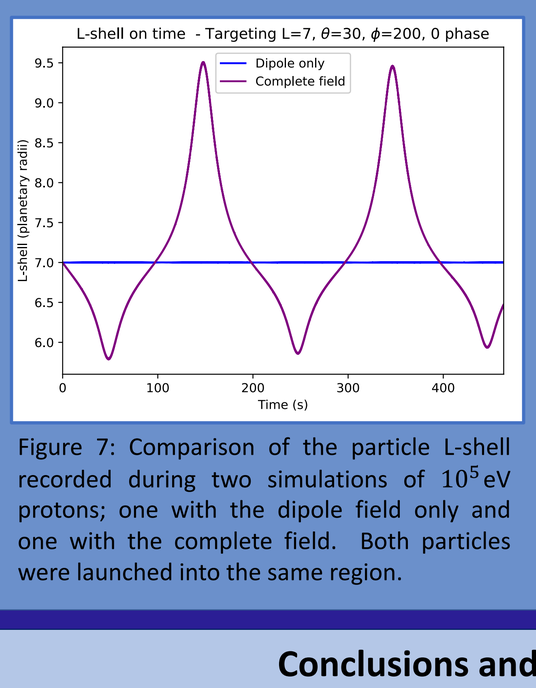

Figure 7: Comparison of the particle L-shell recorded during two simulations of 10^5 eV protons; one with the dipole field only and one with the complete field. Both particles were launched into the same region.

Single bounce runs

- For both protons and electrons, our preliminary results (figure 8) show a large change in L-shell at the equator after one `bounce' but only when the quadrupole component is present.
- There is a much greater deviation for protons, as expected, since they have a larger gyro-radius, and so experience more changes in the magnetic field along one gyration and therefore experience more radial drift.
- Electrons show deviation in the opposite direction to protons because of their opposing charge.
- The largest source of error is the truncation in the forward Euler method used to calculate the particle position. All other errors are insignificant in comparison. To reduce this error, for the final results we will reduce the step size. Our early final results match the preliminary results.

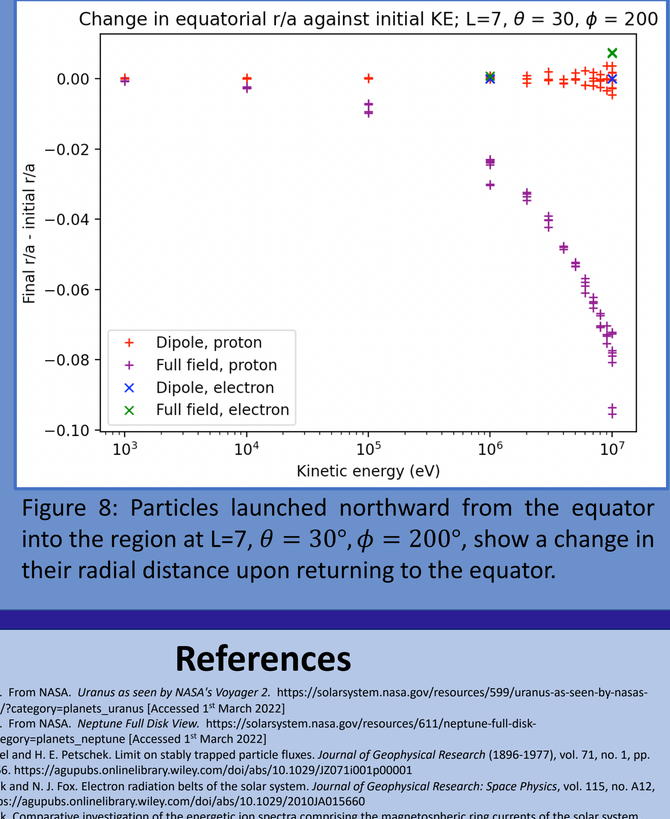

Figure 8: Particles launched northward from the equator into the region at L=7, $\theta = 30°$, $\phi = 200°$, show a change in their radial distance upon returning to the equator.

6 Conclusions and Implications

- We have shown evidence suggesting that the large quadrupole moment in the magnetic field of Uranus and Neptune can influence the protons in the radiation belts to drift across L shells, potentially leading to the proton deficiency observed by Voyager 2.
- As our results do not take into account the effects of multiple reflections and the inter-particle interactions within the radiation belts, a more complex numerical scheme is necessary to properly assess the scale of the effect we have found.
- This was the first step in understanding one of the driving forces behind the particle intensity of the ice giants' radiation belts, which is essential in the design of any new flagship mission visiting the outermost planets of our solar system.

7 References

1. NASA/JPL. From NASA. *Uranus as seen by NASA's Voyager 2*. https://solarsystem.nasa.gov/resources/599/uranus-as-seen-by-nasas-voyager-2/?category=planets_uranus [Accessed 1st March 2022]
2. NASA/JPL. From NASA. *Neptune Full Disk View*. https://solarsystem.nasa.gov/resources/611/neptune-full-disk-view/?category=planets_neptune [Accessed 1st March 2022]
3. C. F. Kennel and H. E. Petschek. Limit on stably trapped particle fluxes. *Journal of Geophysical Research* (1896-1977), vol. 71, no. 1, pp. 1–28, 1966. https://agupubs.onlinelibrary.wiley.com/doi/abs/10.1029/JZ071i001p00001
4. B. H. Mauk and N. J. Fox. Electron radiation belts of the solar system. *Journal of Geophysical Research: Space Physics*, vol. 115, no. A12, 2010. https://agupubs.onlinelibrary.wiley.com/doi/abs/10.1029/2010JA015660
5. B. H. Mauk. Comparative investigation of the energetic ion spectra comprising the magnetospheric ring currents of the solar system. *Journal of Geophysical Research: Space Physics*, vol. 119, no. 12, pp. 9729–9746, 2014. https://agupubs.onlinelibrary.wiley.com/doi/abs/10.1002/2014JA020392
6. NASA. From Wikipedia. *Van Allen Radiation Belt*. https://commons.wikimedia.org/wiki/File:Van_Allen_radiation_belt.svg
7. F. Herbert, "Aurora and magnetic field of Uranus," Journal of Geophysical Research: Space Physics, vol. 114, (A11), pp. n/a, 2009. Available: https://api.istex.fr/ark:/67375/WNG-TT30FDTT-J/fulltext.pdf. DOI: 10.1029/2009JA014394.
8. J. E. P. Connerney, "Magnetic fields of the outer planets," Journal of Geophysical Research: Planets, vol. 98, (E10), pp. 18659-18679, 1993. Available: https://api.istex.fr/ark:/67375/WNG-9Z0K9SVH-S/fulltext.pdf. DOI: 10.1029/93JE00980.
9. P. K. Soni, B. Kakad and A. Kakad, "L-shell and energy dependence of magnetic mirror point of charged particles trapped in Earth's magnetosphere," Earth Planets Space, vol. 72, (1), pp. 1-15, 2020. Available: https://link.springer.com/article/10.1186/s40623-020-01264-5. DOI: 10.1186/s40623-020-01264-5